



## Green Synthesis of Silver Nanoparticles Using Green Tea Extract and Evaluation of Their Antiviral Potential against Foot-and-Mouth Disease Virus Serotype O: An In-Vitro Study



Gabr F. EL Bagoury<sup>1</sup>, Ayman H. Mahmoud<sup>2</sup>, Samr Kassem<sup>3</sup> and Rawan Elhabashy<sup>4\*</sup>

<sup>1</sup>Department of Virology, Faculty of Veterinary Medicine, Benha University, Toukh 13736, Egypt.

<sup>2</sup>Biotechnology Research Department, Animal Health Research Institute, Dokki 12618, Agricultural Research Center, Giza 12619, Egypt.

<sup>3</sup>Nanomaterials Research and Synthesis Unit, Animal Health Research Institute, Agricultural Research Centre, Giza 12618, Egypt.

### Abstract

**F**OOT-AND-MOUTH disease (FMD), is an economically significant viral disease on a global scale. As a result, effective virus control methods must be implemented, including novel FMD antivirals. Herein, we synthesized silver nanoparticles (Ag-NPs) using green tea (GT) extracts as a reducing agent and evaluated their anti-FMDV efficacy. Green tea silver nanoparticles (GT Ag-NPs) synthesis was confirmed using transmission electron microscopy (TEM) analysis, Fourier transform infrared (FT-IR) spectroscopy, and dynamic light scattering (DLS). The TEM revealed distinctive single spherical NPs, with a particle size of 15.1-16.9 nm, while DLS revealed an average particle size of 28.86 nm. NPs' cytotoxicity was initially assessed on the baby hamster kidney cells (BHK-21) using an MTT (3-[4, 5-dimethylthiazole-2-yl]-2, 5-diphenyl 2H-tetrazolium bromide) colourimetric method. Consequently, a viral yield reduction assay detected by 50% tissue culture infectious dose (TCID<sub>50</sub>), and a cytopathic effect inhibition assay detected by an MTT was performed to check the non-cytotoxic concentrations' antiviral potential at different infection times. Results disclosed promising FMDV inhibitory effects; the pre-infection led to 31.75% virus titer reduction, and the 50% inhibitory concentration (IC<sub>50</sub>) and selectivity index (SI) values were 2.45 µg/mL and 66.5, respectively. During post-infection, the greatest viral inhibition activity was detected with a 45.97% reduction; the IC<sub>50</sub> and SI values were 2.05 µg/mL and 79.5, respectively. However, no inhibitory action was observed during the virucidal process, suggesting that GT Ag-NPs can suppress FMDV replication, particularly in the early phases, and cannot exert a direct virucidal effect. The current work demonstrates the green synthesized Ag-NPs anti-FMDV capability in vitro.

**Keywords:** Green chemistry, RNA virus, MTT assay, Cytopathic inhibition assay, TCID<sub>50</sub>.

### Introduction

Foot-and-mouth disease (FMD) is an economically, socially devastating, and highly contagious viral disease that affects more than 70 cloven-hoofed animals (e.g., African buffaloes, sheep, cattle, goats, and pigs), and many other non-domesticated species [1]. FMD virus (FMDV) is responsible for FMD, which is a positive single-stranded RNA virus belonging to the family *Picornaviridae*, genus *Aphthovirus*, and has been categorized into seven antigenically different serotypes (O, A, C, SAT 1, SAT

2, SAT 3, and Asia 1) in addition to various subtypes with no cross-protection [2]. The FMDV infection causes an acute disease with significant morbidity but low mortality, accompanied by fever, lameness, and vesicles on the feet, mouth, snout, and teats [3].

FMD is still spreading worldwide across many countries in Asia, Africa, and the Middle East [4]. In Egypt, the disease is enzootic with three FMDV serotypes: A, O, and SAT2, posing the greatest threat to susceptible animals [5]. FMDV spreads mainly by aerosol droplets via close contact in infected animal groups. FMD control and eradication are extremely

\*Corresponding author: Rawan Elhabashy, E-mail: dr.rawan1990@hotmail.com. Tel.: +20 1148730104

(Received 04 August 2024, accepted 20 December 2024)

DOI: 10.21608/EJVS.2024.309594.2289

©National Information and Documentation Center (NIDOC)

difficult due to its high contagiousness, rapid spread, wide geographical distribution, broad host spectrum, and serotype diversity [6].

However, disease control is achieved with the vaccination of susceptible animals with an inactivated vaccine, animal movement restriction, and early detection of outbreaks to prevent further spread of the disease [7].

Nanoparticles (NPs) have evolved as an alternate option due to their improved diagnostic and therapeutic uses in medicine. They have significant advantages, including their small diameter, high surface area, remarkable physical and chemical properties, and the potential to incorporate multiple antiviral medications onto the same nanoparticle. Consequently, new antiviral therapy techniques based on Nanomaterials have been presented [8].

Metal NPs have been proposed as prospective antiviral alternatives because metals may attack a broad range of viral locations and interrupt infections. They modulate the host immune system's response to invading microorganisms, relieve symptoms, and are less likely to lead to resistance development compared to typical antivirals [9].

Ag-NPs, in particular, are gaining popularity due to their unique physical, chemical, and biological properties along with powerful antibacterial and antiviral properties [10], especially against FMDV [11]. Various methods for the synthesis of NPs have been developed, each having its own set of advantages and limitations. The biological approach has been applied in nanoparticle synthesis to compensate for these physical and chemical limitations, such as toxicity and high cost [12].

The green chemistry that involves the use of plant extracts is simple, economical, efficient, and environmentally safe. Herbal plants provide a wide range of natural compounds with potent antiviral action. One of these phytochemicals is GT-derived polyphenols Epigallocatechin-3-gallate (EGCG), which has been previously reported to exert antiviral activities against various viruses, especially positive-sense single-stranded RNA viruses. In addition, they have anti-oxidative, anti-inflammatory, and antibacterial properties [13]. Recently, natural extracts with antiviral activity have been shown to function as reducing and stabilizing agents. When combined with nanotechnology, this provides a novel way to combat viral diseases [14].

Considering this, the present study aimed to synthesize Ag-NPs from GT extract as a reducing and stabilizing agent in nanoparticle formulation in an environment-friendly method without any additional

reducing chemical agents. Additionally, it evaluates the prepared NPs' antiviral efficacy against FMDV serotype O in BHK-21 cells.

## **Material and Methods**

### *Green synthesis of GT-Ag NPs*

All chemicals and plant extract precursors used in the synthesis of Ag-NPs were purchased from Sigma-Aldrich, (UK). GT was obtained from a local market (Imtenan, Egypt). Silver nitrate ( $\text{AgNO}_3$ ), polyethylene glycol, and sodium hydroxide (NaOH) were purchased from Sigma-Aldrich, (UK).

GT is extracted by dissolving 2 g of dried, grinded GT leaves in 100 ml of deionized water. The mixture was heated for 30 min at 60°C under continuous magnetic stirring, then cooled at room temperature and filtered by Whatman No.1 filter paper. GT Ag-NPs were synthesized by adding 75 ml of  $\text{AgNO}_3$  (0.01 M/ 100 mL/ 0.16987 g) to 75 ml of green tea extract in dropwise under continuous stirring. Before  $\text{AgNO}_3$  titration, ethylene glycol was added at 0.1% (v/v, 7.5 mL) to the GT solution. The pH of the final solution was adjusted by dropping NaOH at 1 M until reaching 10.5; the solution was then heated for 30 minutes at 50°C to increase the yield of GT Ag-NPs. Finally, the obtained NPs were centrifuged at (12000 rpm, 15 min), washed three times with deionized water to purify GT-Ag-NPs of unreacted materials, and then dried at room temperature (30°C).

### *Characterization of green tea-silver nanoparticles (GT Ag-NPs)*

The morphology and size of synthesized NPs were analyzed using a transmission electron microscope (TEM) (JEOL, JEM-2100, USA). Fourier transform infrared spectroscopy (FT-IR) at the scanning range of 4000-400  $\text{cm}^{-1}$  (Perkin Elmer, UK) was applied for the green tea and synthesized GT Ag-NPs to identify the chemical composition and interaction between the functional groups involved in the synthesis and capping of Ag-NPs. The particle size and surface charge potential of the GT Ag-NPs were detected by dynamic light scattering (DLS), Nanotracer-Wave Zetasizer (Microtrac, USA).

### *Cell lines and virus*

BHK-21 cells (VACSERA Research Foundation, Giza, Egypt) were cultured in Dulbecco's Modification of Eagle's Medium (DMEM) supplemented with 10% or 2% fetal bovine serum (FBS) to prepare growth or maintenance medium, respectively, and 0.1% antibiotic/antimycotic solution. The cells were maintained at 37°C (5%  $\text{CO}_2$ ). All medium components were filtered and sterilized using a 0.22  $\mu\text{m}$  syringe

filter. They were provided by (Gibco-BRL, Grand Island, NY, USA), in addition to trypsin-EDTA.

FMDV serotype O (O/ME-SA/ Sharquia-72) was used to investigate the antiviral activity of NPs. The endpoint dilution, expressed as 50% tissue culture infectious dose (TCID<sub>50</sub>), was measured with the Reed and Muench formula [15]. For cytotoxicity and antiviral assays, GT-Ag NPs were prepared in a maintenance medium, sonicated for 1 min, and then sterilized by UV for 30 min before use.

#### *Cytotoxicity determination*

To assess the cytotoxicity of synthesized Ag-NPs, an MTT assay was performed. BHK-21 cells were seeded into a 96-well culture plate ( $2 \times 10^4$  cells/well) and left at 37°C in a 5% CO<sub>2</sub> incubator for 24 hours (hrs) until a confluent sheet was obtained. A range of concentrations (0.98-2000 µg/ml) (2-fold serial dilution) of GT-Ag NPs diluted in maintenance medium were added in triplicate in parallel with the cell controls (non-NPs treated cells) and incubated at 37°C (5% CO<sub>2</sub>) for 48 hr. Next, the medium was removed, cells were washed with phosphate-buffered saline (PBS), and 20 µL of 5 mg/mL MTT dissolved in PBS was added. The formazan crystals were then dissolved with dimethylsulfoxide (DMSO). The optical density (OD) was measured at 560 nm, and cell viability was expressed as the percentage of absorbance of the treated cells relative to that of the control cells, taking the mean value performed in triplicate. The 50% cytotoxic concentration (CC<sub>50</sub>), defined as the compound concentrations that reduce the number of viable cells by 50%, was calculated through MasterPlex 2010 software pack (MiraiBio Group, Hitachi Solutions America, Ltd.).

#### *Antiviral activity evaluations*

The antiviral activity of NPs was conducted in three sections: pre-viral infection NPs treatment, post-viral infection NPs treatment, and virucidal treatment with some modifications during each process. The GT Ag-NPs were introduced to BHK-21 cells at different periods relative to the virus infection cycle in order to determine at which stage of the virus infection cycle NPs can act. All the steps were assessed using two methods: virus yield reduction assay detected by TCID<sub>50</sub>, and cytopathic effect inhibition assay detected by an MTT.

#### *Virus yield reduction assay*

For the pre-viral infection treatment, BHK-21 cells were cultivated in a 96-well plate at 37°C in a 5% CO<sub>2</sub> incubator until confluence. The growth media were removed. Next, 0.1 ml of GT Ag-NPs (15.63 µg/ml) was added to cells for 2 hrs at 37°C (5% CO<sub>2</sub>). The

supernatants were then removed and followed by infection with 0.1 ml of ten-fold serial dilutions of virus stock suspension in maintenance media, and further incubated for 48 hrs at 37°C (5% CO<sub>2</sub>). To perform the post-viral infection treatment, BHK-21 cells were infected with various ten-fold serial dilutions of virus stock suspension in maintenance media for 2 hrs at 37°C (5% CO<sub>2</sub>). Next, the supernatants were removed, and cells were incubated with 0.1 ml of Ag-NPs (15.63 µg/ml) for 48 hr at 37°C in a 5% CO<sub>2</sub> incubator. For the virucidal infection treatment, 0.1 ml of Ag-NPs (15.63 µg/ml) concomitant with 0.1 ml of each concentration of virus ten-fold serial dilutions were incubated for 2 hrs at 37°C (5% CO<sub>2</sub>). These mixtures have been introduced to the cells and incubated for 48 hrs at 37°C in a 5% CO<sub>2</sub> incubator to recognize the direct effect of NPs on the virus.

All experiments were conducted in triplicates in parallel with the virus controls with various ten-fold serial dilutions (virus-infected, non-NPs-treated cells). After 48 hrs, the cells were monitored for FMDV-induced cytopathic effect (CPE). The neutralization power of the tested NPs was determined by the reduction of the virus titer related to the control, using the TCID<sub>50</sub> of treated and untreated virus according to [16] and expressed by the Reed and Muench formula [15].

#### *Cytopathic effect inhibition assay*

The antiviral activity of synthesized Ag-NPs against FMDV was determined using an MTT-based cytopathic effect inhibition assay, which monitored CPE and allowed the percentage of cell viability to be calculated according to [17] through the following protocol: For the pre-viral infection treatment, a confluent monolayer of BHK-21 cells was allowed to grow for 24 hrs in a 96-well plate. Cells then were incubated with 0.1 ml of GT Ag-NPs (two-fold diluted concentration range of 15.63-1.95 µg/ml) in triplicates for 2 hrs at 37°C (5% CO<sub>2</sub>). The supernatants were then removed and followed by infection with 0.1 ml of diluted virus suspension containing the TCID<sub>50</sub> of virus stock. This dose was selected to produce the desired CPE 48 hrs after infection.

In parallel, the virus controls (virus-infected, non-NP-treated cells) and cell controls (non-infected, non-NP-treated cells) were incubated at 37°C in 5% CO<sub>2</sub> for 48 hrs. For the post-viral infection treatment, confluent BHK-21 cells in a 96-well plate were infected at 37°C (5% CO<sub>2</sub>) for 2 hrs with 0.1 ml of virus dilution suspension to allow virus penetration. The supernatants were removed, and then overlaid with 0.1 ml of GT-Ag NPs in various concentrations (two-fold diluted concentration range of 15.63-1.95

$\mu\text{g/ml}$ ); the plate was incubated at  $37^\circ\text{C}$  in 5%  $\text{CO}_2$  for 48 hrs. For the virucidal treatment, 0.1 ml of GT Ag-NPs concentrations (two-fold diluted concentration range of 15.63-1.95  $\mu\text{g/ml}$ ) were incubated for 2 hrs at  $37^\circ\text{C}$  (5%  $\text{CO}_2$ ) with an equal volume of virus dilution suspension. Next, mixed suspensions were added to confluent BHK-21. In each treatment, the culture plates were incubated for 48 hr. After 48 hrs, the cells were monitored for CPE.

After each treatment, the cells were washed with PBS, and 20  $\mu\text{l}$  of MTT solution (5 mg/ml stock solution) was added for 4 hr at  $37^\circ\text{C}$ . The medium was aspirated, and the formed formazan crystals were dissolved with DMSO. OD was detected at 560 nm. Data were presented as the mean values of triplicate wells. The MTT technique quantitatively assessed the cytopathic effect caused by virus infection at 48 hr post-infection and allowed the cell viability percentage to be calculated. The 50% inhibitory concentration ( $\text{IC}_{50}$ ), the dose achieving 50% protection, was calculated through the MasterPlex 2010 software pack (MiraiBio Group, Hitachi Solutions America, Ltd.). The ratio of  $\text{CC}_{50}/\text{IC}_{50}$  was calculated to measure the selectivity index (SI) to determine the therapeutic window.

#### Statistical analyses

Data were reported as mean  $\pm$  standard deviation (SD) and performed in triplicate. The significance of differences was analyzed using the Student t-test. Values with (P-value  $\leq 0.05$ ) were considered statistically significant. Microsoft Excel (2010) software produced all statistical analysis and graphical illustrations.

## Results

### Characterization of synthesized (GT Ag-NPs)

#### Average particle size and zeta potential

The obtained results of Dynamic Light Scattering (DLS) demonstrate that the average particle size of synthesized Ag-NPs is 28.86 nm with a narrow size distribution (polydispersity index [PDI] is 0.12), and surface charges of + 18.9 mV (Fig. 1A).

#### FT-IR spectra

FTIR spectra of green tea extract and synthesized GT Ag-NPs were evaluated by linking the absorption bands to the corresponding compounds to investigate the possible phytochemical components and functional groups involved in Ag-NPs reduction and capping.

FT-IR spectra of green tea and synthesized GT-Ag NPs were shown in (Fig. 1B). For GT, the peak at  $3428\text{ cm}^{-1}$  showed the presence of N-H bond in stretching mode present in amines. The peak at  $2918$

$\text{cm}^{-1}$  showed the presence of O-H bond stretching mode in carboxylic acid, while the peak at  $2852\text{ cm}^{-1}$  referred to the presence of C-H stretching in alkanes and O-H stretching in carboxylic acid. The peak at  $1635\text{ cm}^{-1}$  showed the presence of the C=C bond aromatic group and the primary amine group of proteins, while the peak at  $1439\text{ cm}^{-1}$  showed the presence of the C-O-H bond in bending mode. The peak at  $1031\text{ cm}^{-1}$  showed the presence of the C-O bond in the stretching mode of alcohol in polyphenols and ether, while the peak at  $572\text{ cm}^{-1}$  represented the C-Cl stretching bond. However, for synthesized GT-Ag NPs, the N-H bond in stretching mode was represented in the peak of  $3429\text{ cm}^{-1}$ . The peak at  $2918\text{ cm}^{-1}$  showed the presence of O-H bond stretching mode (carboxylic acid), while the peak at  $2852\text{ cm}^{-1}$  referred to the presence of C-H stretching in alkanes and O-H stretching bonds in carboxylic acid. The peak at  $1632\text{ cm}^{-1}$  referred to the presence of the C=C bond of the aromatic group, while the peak at  $1052\text{ cm}^{-1}$  indicated the presence of the C-O bond in the stretching mode of alcohol and ether. The peak at 607, 452, and  $417\text{ cm}^{-1}$  showed the presence of a C-Cl bond in stretching mode.

#### Morphological characters

TEM images of stabilized GT Ag-NPs were shown in (Fig. 1C). Distinctive single NPs without aggregation were observed, as well as a spherical shape. The size ranged from 15.1 to 16.9 nm.

#### Nanoparticles non-toxic concentrations

Cytotoxic effects of synthesized GT Ag-NPs on BHK-21 cells were evaluated by the colourimetric MTT assay based on the intensity of color change after the reduction of tetrazolium dyes by mitochondrial enzymes. This was done to ensure that the tested GT Ag-NPs concentrations are not toxic and to exclude the probability that NPs cytotoxicity affects FMDV infectivity. The cell viability percentage was determined to be greater than 90% when the cells were treated with Ag-NPs concentrations of 31.25, 15.63, 7.81, 3.91, 1.95, and 0.98  $\mu\text{g/mL}$  with no significant cytotoxic effects toward BHK-21 cell line. The 50% cytotoxicity concentration ( $\text{CC}_{50}$ ) for GT Ag-NPs was obtained at  $163\mu\text{g/mL}$  (Fig. 2).

#### Antiviral activity

##### Virus yield reduction assay

To explore the reduction in FMDV yield by synthesized GT Ag-NPs, the tested NPs concentration ( $15.63\text{ }\mu\text{g/ml}$ ) was added to ten-fold serial dilutions of virus in three different treatments as discussed above and assessed by the  $\text{TCID}_{50}$  with the Reed and Muench method. The results of the pre-viral infection

experiment showed a significant reduction in the virus yield with a titer reduction of 2.01 log<sub>10</sub> TCID<sub>50</sub> (from 10<sup>6.33</sup> to 10<sup>4.32</sup> TCID<sub>50</sub>/mL) and a 31.75% reduction per cent when compared to the virus control. Also, the post-viral infection experiment showed a significant reduction in the virus yield with a titer reduction of 2.91 log<sub>10</sub> TCID<sub>50</sub> (from 10<sup>6.33</sup> to 10<sup>3.42</sup> TCID<sub>50</sub>/mL) and a 45.97% reduction per cent when compared to the virus control. Meanwhile, the virucidal infection experiment did not show any significant differences compared to the control group with a titer reduction of 0.23 log<sub>10</sub> TCID<sub>50</sub> (from 10<sup>6.33</sup> to 10<sup>6.1</sup> TCID<sub>50</sub>/mL) and 3.63% reduction percent (Fig. 3). Taken together, these results showed significant antiviral activity against FMDV in pre- and post-treatment (*P*-value ≤ 0.05). In contrast, the anti-FMDV activity of Ag-NPs was more prominent during the post-infection stage of the virus than at the pre-infection stage, suggesting that the synthesized Ag-NPs exert an inhibitory effect on FMDV replication in the target cells. However, no antiviral activity was in the virucidal treatment, proposing that the NPs did not exhibit direct inactivation on the free virus.

#### *Cytopathic inhibition assay*

The antiviral potential of synthesized GT Ag-NPs on FMDV infection in BHK-21 cells was calculated by measuring cell viability percentage using the results of the MTT assay. In the pre-viral infection stage, the cells were treated with NPs before virus inoculation. Significant increases in cell viability percentages were obtained at 67.86%, 64.62%, 58.87%, and 46.26% in the cells treated with 15.63, 7.82, 3.91, 1.95 µg/mL, respectively, when compared to the virus control (*P*-value ≤ 0.05) (Fig. 4A). In the post-viral infection stage, the cells were treated with NPs 2 hrs. after infection. Significant increases in cell viability percentages were obtained at 84.92%, 66.66%, 59.52%, and 49.60%, in the cells treated with 15.63, 7.82, 3.91, and 1.95 µg/mL, respectively, when compared to the virus control (*P* ≤ 0.05) (Fig. 4B). However, virucidal treatment did not show a significant cell viability percentage. Cell viability percentages of 31.33%, 30.32%, 29.94%, and 29.85% were obtained in cells treated with 15.63, 7.82, 3.91, and 1.95 µg/mL, respectively, when compared to the virus control (*P* ≤ 0.05) (Fig. 4C). Cell viability percentages in the negative control (untreated cells) and viral control were 100% and 28.65%, respectively. The IC<sub>50</sub> and SI values were calculated to be 2.45 µg/mL and 66.5, respectively, in the pre-treatment, while 2.05 µg/mL and 79.5, respectively, in the post-treatment.

The results of the cytopathic inhibition assay indicated that antiviral activity in the pre- and post-

viral infection treatment had a dose-dependent effect. However, the anti-FMDV activity of GT Ag-NPs was greater in the post-viral infection treatment than the pre-treatment, suggesting that GT Ag-NPs have an antiviral effect at the early stages of FMDV replication. Meanwhile, virucidal activity was not recorded at any NPs concentrations, proposing that NPs could not act directly against FMDV, resulting in viral inactivation. In all steps, the results of the virus yield reduction assay were concurrent with those of the cytopathic inhibition assay detected by an MTT.

#### **Discussion**

Ag-NPs have antimicrobial properties and are excellent candidates for the development of new antivirals [18]. GT has been shown to have antiviral properties, and involving GT in NPs synthesis as a natural and readily available source could be a step forward in antiviral therapies [19]. Based on this, the current study was designed to synthesize Ag-NPs utilizing GT as a reducing agent and investigate their potential antiviral activity for FMDV in vitro.

Synthesized GT Ag-NPs were characterized to determine their formation, morphology, and stability. The most important features of an NPs system are particle size and size distribution, as they determine NPs intracellular absorption and toxicity [20], in addition to Z potential, which affects NPs stability [21]. DLS showed a narrow size distribution (PDI) of 0.12, and surface charges of + 18.9 mV (Fig. 1A). TEM confirmed the presence of non-aggregated distinctive single NPs with spherical morphology and a size ranging from 15.1-16.9 nm (Fig. 1C). Previous researchers have identified green synthesized Ag-NPs within a size range of 15-33 nm [22]. The antiviral efficacy of NPs is size-dependent; the smaller the size of NPs, the greater their viral interaction and inhibition, due to their larger surface area as well as their ability to enter the host cell and virus genome, thereby blocking replication.

However, the separate single NPs without agglomeration detected by TEM can be explained by the stabilizing action of phytochemicals present in the GT extract [22, 23] as well as polyethylene glycol that was added as a capping agent. Capping agents increase NPs' efficacy and ensure higher interaction than bare ones, as they improve stability and reduce agglomeration and potential cytotoxicity by preventing direct contact of the metal with the cells [24].

The FTIR data denote the presence of bioactive compounds that mediate the GT Ag-NP synthesis and stabilization, like polyphenols, amines, alkanes, polysaccharides, and proteins. However, by comparing the GT and synthesized Ag-NPs FTIR spectra (Fig.

1B), changes in their chemical components can be identified as the nanoparticles were encapsulated. These characterization results are in line with a related study involving the green synthesis of Ag-NPs using GT extract [22].

Synthesized GT-Ag NPs were safe at a concentration of up to 31.25 µg/ml and  $CC_{50}$  163 µg/ml (Fig. 2). Our results were in line with the outcomes of [18], who reported no significant toxicity at similar concentrations of green synthesized Ag-NPs from medicinal plants; however, the reason of Ag-NPs cytotoxicity may be attributed to the release of silver ions and formation of reactive oxygen species that led to cell apoptosis, as well as the NPs size; smaller particles are more toxic because of the increased surface area of interaction and their easy diffusion into the cells [25]. Generally, the variability of Ag-NPs cytotoxicity is dependent on the cell type, method of preparation, concentrations, coating, and characterization of NPs [16].

Free FMD viruses attach to cell receptors and then lose their capsid upon cell entrance. The single-stranded RNA genome is transported to the cytoplasm to be a template for creating a new genome, as well as for protein synthesis. The new viral genome replicates are subsequently encased in a new capsid, giving newly generated virions that gather in the cytoplasm, lyse the cell, and are eventually expelled [26]. To explore the effect of synthesized GT Ag-NPs on extracellular and intracellular FMDV, the virus was treated at various phases of replication with NPs. At each phase, the antiviral activities of NPs were measured in terms of inhibition of virus replication and increase of cell viability percentage.

In the pre-treatment assay, cells were treated with GT Ag-NPs before virus infection to assess the ability of Ag-NPs' pre-treated cells to resist the viral infection, and effective results were obtained, as evidenced by the significant drop in viral load (31.75% reduction percent) along with significant protection for cells from CPE ( $IC_{50}$  of 2.45 µg/mL and SI of 66.5) (Fig. 3; Fig. 4A). Accordingly, it may be hypothesized that Ag-NPs may alter the virus's attachment to the cell receptor by covering the cell surface or interfere with the virus's passageway into cells, reducing its ability to infect the host cells [16].

In the post-treatment assay, the cells were treated with GT Ag-NPs 2 hr after infection to determine Ag-NPs' capability to inhibit the virus in previously infected cells. In this step, the highest anti-FMDV activity was recorded than the pre-viral infection, with significant decrease in viral load (45.97% reduction per cent) and the lowest  $IC_{50}$  of 2.05 µg/mL and SI of 79.5 (Fig. 3, Fig. 4B), postulating that Ag-NPs exert

potent antiviral activity in vitro at the initial phase of FMDV infection cycle, by targeting an event after viral entry in BHK-21 cells, or may correspond with the onset of intracellular viral RNA production according to results obtained by [26].

Meanwhile, the virucidal infection assay can elucidate if the Ag-NPs can directly inactivate free viruses. Unlike earlier steps, the results revealed no significant reduction in viral infectivity or significant increase in cell viability percentage in the treated cells at any non-toxic concentrations of GT Ag-NPs (Fig. 3; Fig. 4C), implying that GT Ag-NPs cannot directly inhibit the free extracellular FMDV. Similar findings were recorded in the case of [27], who reported the in-vitro antiviral activity of green-synthesized Ag-NPs against PPRV where a significant viral titers reduction was detected only when the NPs were applied in the pre-viral infection step, or at 1- 2 hrs post-infection with no virucidal effect, indicating that the green-synthesized Ag-NPs exclusively affect the early stages of the PPRV life cycle. SI measures the drug's safety margin. When the index value approaches one, safety is reduced, and hence, drug usage is extremely dangerous [21]. Herein, the results are promising because of the low  $IC_{50}$  and high SI achieved against FMDV.

The antiviral activity of green-synthesized NPs has primarily been studied using Ag-NPs [14, 18]. Ag-NPs have been reported to inhibit several stages of the virus-host cell interaction and may act on many targets at the same time [27]. Herein, the antiviral results suggested that early stages of the FMDV replication cycle (from the time of pre-infection until 2 hrs after infection) are affected by the Ag-NPs, observing a greater significant effect at 2 hrs after infection. Considering the Ag-NPs' probable mechanism against RNA viruses as demonstrated by other authors, these antiviral findings may be hypothesized due to the blocking of cellular receptors, disrupting the adhesion of viral particles to host cells, thus inhibiting infection, impeding the critical pathways needed for virus replication, as well as interaction with virus genome [14, 25, 28]. Additionally, the observed anti-FMDV effect is due to the GT, which has reducing, capping, and antiviral properties. EGCG, a main phytoconstituent found in GT, is a broad-spectrum antiviral drug with distinct mechanisms at different stages of the viral cycle.

Furthermore, it exhibits anti-inflammatory and prophylactic properties. Some researchers suggest encapsulating EGCG with nanoparticles to improve its efficacy and bioavailability [29]. To summarize, the remarkable efficacy of green-synthesized NPs provides new promise for the development of new antiviral

therapies against different viruses, and the exact mechanism of action should be explored further in detail for better efficacy.

### **Conclusion**

Stable GT Ag-NPs were synthesized in a clean, cost-effective manner utilizing GT as a reducing agent. Evaluating the NPs' antiviral capability indicated that GT Ag-NPs could suppress FMDV replication primarily during the early phases of infection, including the pre-viral infection phase and 2 hrs post-infection, with striking antiviral effects during post-infection. Thus, it is proposed that the early time of the FMDV replication stage is the target for the antiviral effect of GT Ag-NPs. However, it cannot exert a direct extracellular virucidal effect, anticipating its role as a potential anti-FMDV agent. Our findings expand the

scope of future in vivo research, as well as exploring GT Ag-NPs' ability to suppress other RNA viruses.

### *Acknowledgments*

Not applicable.

### *Funding statement.*

This study didn't receive any funding support

### *Declaration of Conflict of Interest*

This research did not receive any specific grant from funding agencies in the public, commercial, or not-for-profit sectors.

### *Ethical of approval*

Not applicable.

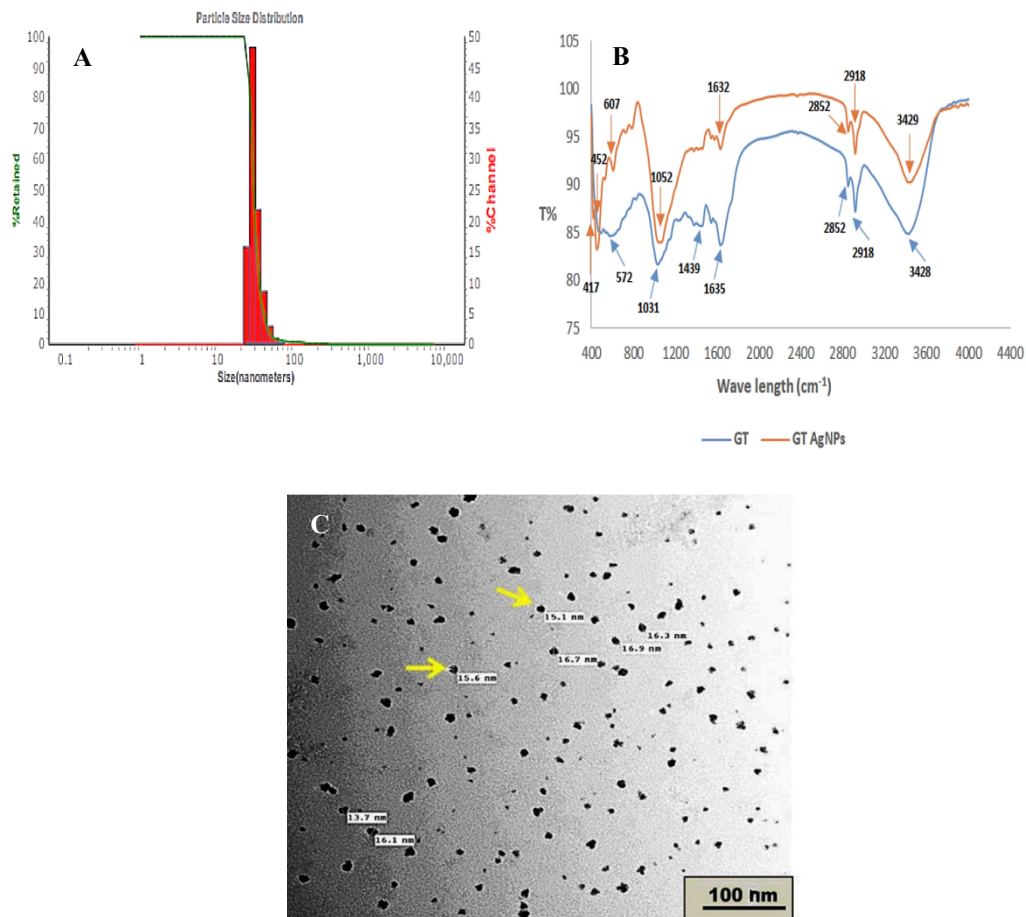


**Fig. 1.** Characterization of GT AgNPs. (A) Particle size pattern of synthesized NPs showing size distribution of 28.86 nm and PDI of 0.12. (B) FT-IR spectra of GT Ag- NPs compared with GT (green tea) at the scanning range of 4400-400  $\text{cm}^{-1}$ . (C) TEM imaging showed well- dispersed nanosphere particles and a size ranging from 15.1 to 16.9 nm, Scale bar = 100 nm.

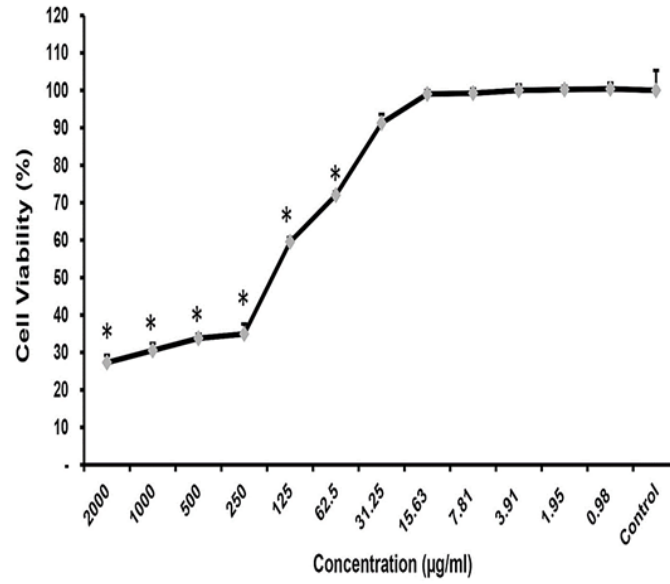


Fig. 2. The cytotoxic effects of tested NPs concentrations against the BHK-21 cell line. The cells were treated with different concentrations of synthesized Ag-NPs (2-fold serial dilutions) for 48 h, in parallel with the cell controls (non-NPs treated cells). Relative cell viability percentage was determined by MTT assay. Concentrations were plotted against cell viability response. Data are expressed as the mean  $\pm$  SD performed in triplicate. Error bars represent the confidence interval for the mean ( $n = 3$ ). \* Statistically significant ( $p \leq 0.05$ ).

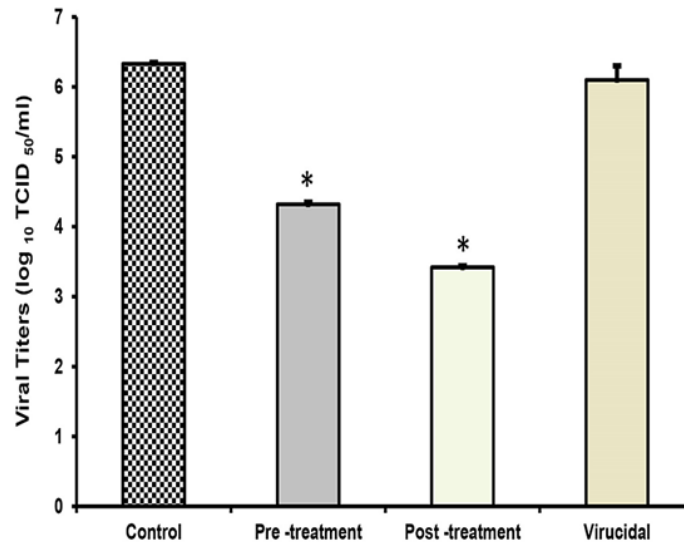
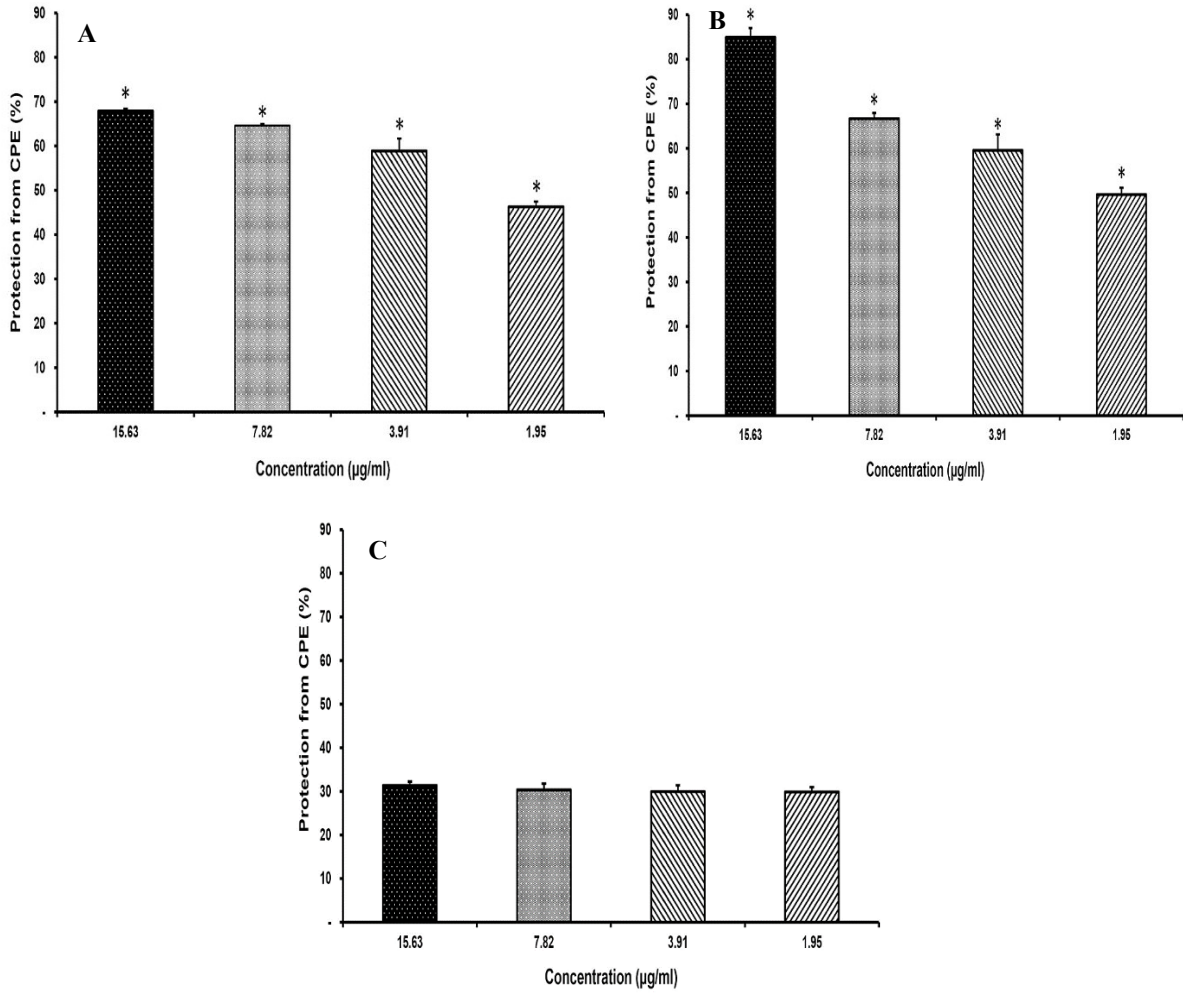


Fig. 3. Virus Yield Reduction assay; determination of viral titers on BHK-21 cells in three different NPs treatments. Virus control (virus-infected, non-NPs-treated cells). TCID<sub>50</sub> was analyzed by the Reed and Muench method. Data are means  $\pm$  SD performed in triplicate.





**Fig. 4.** Effect of synthesized Ag-NPs on inhibition of FMDV in BHK-21 cell line, antiviral effects were detected by a cytopathic inhibition assay using the MTT (A) Pre-treatment assay: confluent BHK-21 cells treated with non-cytotoxic concentrations of synthesized Ag-NPs for 2 hrs at 37 °C and then infected with virus suspension (B) Post-treatment assay: confluent BHK-21 cells infected with virus for 2 hrs at 37 °C and then treated with synthesized Ag-NPs concentrations and (C) Virucidal treatment assay: synthesized Ag-NPs concentrations were mixed with the virus and incubated for 2 hrs at 37 °C then introduced to cells. Results are expressed as mean  $\pm$  SD performed in triplicates. Error bars represent the confidence interval for the mean (n = 3). \* Statistically significant ( $p \leq 0.05$ ).

**References**

1. Li, S.F., Gong, M.J., Sun, Y.F., Shao, J.J., Zhang, Y.G. and Chang, H.Y. In vitro and in vivo antiviral activity of mizoribine against foot-and-mouth disease virus. *Molecules*, **24**, 1723 (2019).
2. Kim, J.W., Kim, M., Lee, K.K., Chung, K.H. and Lee, C.S. Effects of graphene oxide-gold nanoparticles nanocomposite on highly sensitive foot and mouth disease virus detection. *Nanomaterials* , **10**, 1921 (2020).
3. Díaz-San Segundo, F., Weiss, M., Perez-Martín, E., Koster, M.J., Zhu, J., Grubman, M.J. and De los Santos, T. Antiviral activity of bovine type III interferon against foot-and-mouth disease virus. *Virology*, **413**, 283-292 (2011).
4. Thomson, G.R., Vosloo, W., Bastos, A.D.S. Foot and mouth disease in wildlife. *Virus Research*, **91**, 145-161(2003).
5. El Nahas, A.F., Abd El Naby, W.S., Khatab, S.A., Fergany, A.Z.A. and Rashed, R.R. Comparative expression analysis of inflammatory and immune-related genes in cattle during acute infection with foot-and-mouth disease virus in Egypt. *Journal of Veterinary Research*, **65**, 39-44 (2021).
6. Chakraborty, S., Kumar, N., Dhama, K., Verma, A.K., Tiwari, R., Kumar, A. and Singh, S.V. Foot-and-mouth disease, an economically important disease of animals. *Advances in Animal and Veterinary Sciences*, **2**,1-18 (2014).
7. Knight-Jones, T.J., Robinson, L., Charleston, B., Rodriguez, L.L., Gay, C.G., Sumption, K.J. and Vosloo, W. Global Foot-and-Mouth Disease Research Update and Gap Analysis: 2 Epidemiology, Wildlife and Economics. *Transboundary and Emerging Diseases*, **63**,14-29 (2016).
8. Milovanovic, M., Arsenijevic, A., Milovanovic, J., Kanjevac, T. and Arsenijevic, N. Nanoparticles in antiviral therapy. *Antimicrobial nanoarchitectonics*. Chapter **14**,383-410 (2017).
9. Abate, C., Carnamucio, F., Giuffrè, O. and Foti, C. Metal-Based Compounds in Antiviral Therapy. *Biomolecules*, **12**, 933 (2022).
10. Morris, D., Ansar, M., Speshock, J., Ivanciuc, T., Qu, Y., Casola, A. and Garofalo, R.P. Antiviral and immunomodulatory activity of silver nanoparticles in experimental RSV infection. *Viruses*, **11**,732 (2019).
11. Rafiei, S., Rezatofghi, S.E., Ardakani, M.R. and Madadgar, O. Restrictive influence of silver nanoparticles on the life cycle of the foot-and-mouth disease virus. *Nanoscience & Nanotechnology-Asia*, **8**, 248-254 (2018).
12. Govarthanan, M., Seo, Y.S., Lee, K.J., Jung, I.B., Ju, H.J., Kim, J.S., Cho, M., Kamala-Kannan, S. and Oh, B.T. Low-cost and eco-friendly synthesis of silver nanoparticles using coconut (Cocos nucifera) oil cake extract and its antibacterial activity. *Artificial Cells, Nanomedicine, and Biotechnology*, **44**,1878-1882 (2016)
13. Mhatre, S., Srivastava, T., Naik, S. and Patravale, V. Antiviral activity of green tea and black tea polyphenols in prophylaxis and treatment of COVID-19: A review. *Phytomedicine*, **85**,153286 (2021).
14. Haggag, E.G., Elshamy, A.M., Rabeh, M.A., Gabr, N.M., Salem, M., Youssif, K.A. and Abdelmohsen, U.R. Antiviral potential of green synthesized silver nanoparticles of *Lampranthus coccineus* and *Malephora lutea*. *International Journal of Nanomedicine*, **14**, 6217-6229 (2019).
15. Reed, L.J. and Muench, H. A simple method of estimating fifty percent endpoints. *American Journal of Epidemiology* **27**, 493-497 (1938).
16. Rafiei, S., Rezatofghi, S.E., Ardakani, M.R. and Rastegarzadeh, S. Gold nanoparticles impair foot-and-mouth disease virus replication. *IEEE Trans. Nanobioscience*, **15**, 34-40 (2015).
17. Barakat, A.B., El-Esnawy, N.A., Allayeh, A.K. and Ghanem, H.E. Antiviral activity of bovine, buffalo and camel yogurt against human rotavirus in vitro. *The Journal of Applied Sciences Research*, **9**,6425-6430 (2013).
18. Sharma, V., Kaushik, S., Pandit, P., Dhull, D., Yadav, J.P. and Kaushik, S. Green synthesis of silver nanoparticles from medicinal plants and evaluation of their antiviral potential against chikungunya virus. *Applied Microbiology and Biotechnology*, **103**, 881-891 (2019).
19. Mhatre, S., Srivastava, T., Naik, S. and Patravale, V. Antiviral activity of green tea and black tea polyphenols in prophylaxis and treatment of COVID-19: A review. *Phytomedicine*, **85**, 153286 (2021).
20. Mohanraj, V. J. and Chen, Y. J. T. J. O. P. R. Nanoparticles-a review. *Tropical Journal of Pharmaceutical Research*, **5**(1), 561-573 (2006).
21. Meléndez-Villanueva, M.A., Morán-Santibañez, K., Martínez-Sanmiguel, J.J., Rangel-López, R., Garza-Navarro, M.A., Rodríguez-Padilla, C. and Trejo-Ávila, L.M. Virucidal activity of gold nanoparticles synthesized by green chemistry using garlic extract. *Viruses*, **11**,1111 (2019).
22. Widatalla, H.A., Yassin, L.F., Alrasheid, A.A., Ahmed, S.A.R., Widdatallah, M.O., Eltilib, S.H. and Mohamed, A.A. Green synthesis of silver nanoparticles using green tea leaf extract, characterization and evaluation of antimicrobial activity. *Nanoscale Advances*, **4**, 911-915 (2022).
23. Geraldles, A.N., da Silva, A.A., Leal, J., Estrada-Villegas, G.M., Lincopan, N., Katti, K.V. and Lugão, A.B. Green nanotechnology from plant extracts: synthesis and characterization of gold nanoparticles. *Advances in Nanoparticles*, **5**, 176. (2016).
24. Khandelwal, N., Kaur, G., Kumar, N. and Tiwari, A. Application of silver nanoparticles in viral inhibition: a new hope for antivirals. *Digest Journal of Nanomaterials and Biostructures*, **9**, 175-186 (2014b).
25. Jeremiah, S.S., Miyakawa, K., Morita, T., Yamaoka, Y. and Ryo, A. Potent antiviral effect of silver nanoparticles on SARS-CoV-2. *Biochemical and Biophysical Research Communications*, **533**,195-200(2020).

26. Goris, N., De Palma, A., Toussaint, J.F., Musch, I., Neyts, J. and De Clercq, K. 2'-C-methylcytidine as a potent and selective inhibitor of the replication of foot-and-mouth disease virus. *Antiviral Research* 73,161-168(2007).
27. Khandelwal, N., Kaur, G., Chaubey, K.K., Singh, P., Sharma, S., Tiwari, A. and Kumar, N. Silver nanoparticles impair Peste des petits ruminants virus replication. *Virus Research*, 190, 1-7 (2014a).
28. Speshock, J.L., Murdock, R.C., Braydich-Stolle, L.K., Schrand, A.M. and Hussain, S.M. Interaction of silver nanoparticles with Tacaribe virus. *Journal of Nanobiotechnology*, 8,19 (2010).
29. Munin, A. and Edwards-Lévy, F. Encapsulation of Natural Polyphenolic Compounds. a Review. *Pharmaceutics*, 3, 793-829 (2011).

## التوليف الأخضر لجسيمات الفضة النانومترية باستخدام مستخلص الشاي الأخضر وتقييم إمكاناتها المضادة للفيروسات ضد النمط المصلي O لفيروس مرض الحمى القلاعية : دراسة في المختبر

جير فكري الباجوري<sup>1</sup>، ايمن حامد محمود<sup>2</sup>، سمر قاسم<sup>3</sup> و روان الحبشى<sup>2</sup>

<sup>1</sup> قسم الفيروسولوجيا، كلية الطب البيطري، جامعة بنها.

<sup>2</sup> قسم البيوتكنولوجي، معهد بحوث الصحة الحيوانية، الدقي، مركز البحوث الزراعية، الجيزة، مصر.

<sup>3</sup> وحدة بحوث وتصنيع المواد النانوية، معهد بحوث الصحة الحيوانية، الدقي، مركز البحوث الزراعية، الجيزة، مصر.

### الملخص

مرض الحمى القلاعية هو مرض فيروسي ذو أهمية اقتصادية على نطاق عالمي. ونتيجة لذلك، يجب تنفيذ طرق فعالة لمكافحة الفيروسات، بما في ذلك الأدوية الحديثة المضادة لفيروس لمرض الحمى القلاعية. هنا، قمنا بتصنيع جسيمات الفضة النانومترية Ag-NPs باستخدام مستخلصات الشاي الأخضر كعامل اختزال وقمنا بتقييم فعاليتها المضادة لمرض الحمى القلاعية. تم تأكيد تخليق الجسيمات النانوية الفضية للشاي الأخضر GT Ag-NPs باستخدام تحليل المجهر الإلكتروني للإرسال TEM وتشتت الضوء الديناميكي DLS ومطيافية تحويل فورييه للأشعة تحت الحمراء FT-IR كشفت TEM عن كروية واحدة مميزة، بحجم جسيم يتراوح بين 15.1-16.9، بينما كشف DLS عن متوسط حجم جسيم يبلغ 28.86 نانومتر. تم تقييم السمية الخلوية لـ NPs ميدنيًا على خلايا كلى الهامستر الصغير BHK-21 باستخدام MTT). ونتيجة لذلك تم إجراء اختبار تقليل العائد ومقايسة تثبيط التأثير الخلوي المكتشف بواسطة TCID<sub>50</sub> للتحقق من الإمكانيات المضادة للفيروسات للتركيزات غير السامة للخلايا في أوقات العدوى المختلفة؛ أدت العدوى المسبقة إلى انخفاض عيار الفيروس FMDV ومؤشر IC<sub>50</sub>. وكشفت النتائج عن تأثيرات مثبطة واحدة لفيروس بنسبة 31.75%، وكانت قيم التركيز المثبط الانتقائية (SI) بنسبة 50% 2.45 ميكروغرام/مل و66.5 على التوالي. خلال فترة ما بعد الإصابة، تم اكتشاف أكبر نشاط تثبيط للفيروس مع انخفاض بنسبة 45.97%؛ وكانت قيم التركيز المثبط الانتقائية (SI) بنسبة 50% 2.05 ميكروغرام/مل و79.5 على التوالي. ومع ذلك، لم يلاحظ أي عمل مثبط أثناء عملية اباداة الفيروسات مباشرة، مما يشير إلى قدرة GT Ag-NPs على قمع فيروس مرض الحمى القلاعية خاصة في المراحل المبكرة، ولا يمكنها ممارسة تأثير مبيد للفيروسات مباشر. مجتمعة.

الكلمات الدالة: الكيمياء الخضراء، فيروسات ال RNA، اختبار ال MTT، اختبار ال Cytopathic inhibition، assay، TCID<sub>50</sub>